3916 *Chem. Mater.* **2010,** *22,* 3916–3925
DOI:10.1021/cm100252r

CHEMISTRY OF MATERIALS
Article

Topotactic Redox Chemistry of NaFeAs in Water and Air and Superconducting Behavior with Stoichiometry Change

Iliya Todorov,[†] Duck Young Chung,[†] Helmut Claus,[†] Christos D. Malliakas,[‡] Alexios P. Douvalis,[§] Thomas Bakas,[§] Jiaqing He,[⊥] Vinayak P. Dravid,[⊥] and Mercouri G. Kanatzidis*[,†,‡]

[†]*Materials Science Division, Argonne National Laboratory, Argonne Illinois 60439,* [‡]*Department of Chemistry, and* [⊥]*Department of Materials Science & Engineering, Northwestern University, Evanston, Illinois 60208, and* [§]*Department of Physics, University of Ioannina, 45110 Ioannina, Greece*

Received January 26, 2010. Revised Manuscript Received April 30, 2010

We report experimental evidence that shows superconductivity in NaFeAs occurs when it is Na deficient. The oxidation of NaFeAs progresses differently in water and in air. In water the material oxidizes slowly and slightly retaining the original anti-PbFCl structure. In air NaFeAs oxidizes topotactically quickly and extensively transforming to the $ThCr_2Si_2$ structure type. Water acts as a mild oxidizing agent on the FeAs layer by extracting electrons and Na^+ cations from the structure, while oxidation in air is more extensive and leads to change in structure type from NaFeAs to $NaFe_2As_2$. The superconducting transition temperature moves dramatically during the oxidation process. Exposed to water for an extended time period NaFeAs shows a substantial increase in T_c up to 25 K with contraction of unit cell volume. $NaFe_2As_2$, the air oxidized product, shows T_c of 12 K. We report detailed characterization of the redox chemistry and transformation of NaFeAs in water and air using single crystal and powder X-ray diffraction, magnetization studies, transmission electron microscopy, Mössbauer spectroscopy, pOH and elemental analysis.

Introduction

The new class of iron arsenide superconductors that is built with anti-PbO-type FeAs layers intercalated with alkali, alkaline earth metals, or PbO-type rare earth oxide layers is under intense investigation since the recent discovery of $LaO_{1-x}F_x$-FeAs with T_c at 26 K.[1] Superconductivity has been found in several compositional systems such as REOFeAs (RE = La, Ce, Pr, Nd, Sm)[1−4] (1111 phase), AFeAs (A = Li, Na)[5−8] with PbFCl structure type (111 phase), and (A/AE)Fe_2As_2 (A = K, Rb, Cs; AE = Sr, Ba)[9−12] (122 phase). Although the highest achievable superconducting temperature in iron arsenides is yet to be determined, the unconventional nature of superconductivity in these compounds is an important issue.[10] The anti-PbO-type FeAs layer is structurally rigid and electronically and magnetically active on doping. Formal valence electron counting reveals that the charge in the FeAs layer is the same in all three systems, namely −1 per FeAs unit. In the REOFeAs and (AE)Fe_2As_2 phases, superconductivity appears after reaching a critical doping concentration, i.e., substituting some of the O atoms by F in the former and substituting some or full of alkaline-earth atoms by alkali (K, Rb, Cs)[5,11] in the latter. The highest T_c was reported at 55 K for samples of $SmO_{1-x}F_xFeAs$[3] for the so-called 1111 phase and at 38 K from $Ba_{1-x}K_xFe_2As_2$[9] for the 122 phase. Superconductivity in the 111 phase was reported in only two compounds, LiFeAs and NaFeAs. The latter are highly air and moisture sensitive and require special handling. For this reason these materials are relatively little studied and are the least understood of the entire iron arsenide family.

The first report on LiFeAs states that Li-rich and Fe-rich compositions could be obtained but not the stoichiometric LiFeAs.[13] Recently, the uncertainty in the location and content of Li atoms has been a critical issue in

*Corresponding author.

(1) Kamihara, Y.; Watanabe, T.; Hirano, M.; Hosono, H. *J. Am. Chem. Soc.* **2008**, *130*, 3296.
(2) Takahashi, H.; Igawa, K.; Arii, K.; Kamihara, Y.; Hirano, M.; Hosono, H. *Nature* **2008**, *453*, 376.
(3) Ren, Z.-A.; Che, G.-C.; Dong, X.-L.; Yang, J.; Lu, W.; Yi, W.; Shen, X.-L.; Li, Z.-C.; Sun, L.-L.; Zhou, F.; Zhao, X.-Z. *Europhys. Lett.* **2008**, *83*, 17002.
(4) Nekrasov, I. A.; Pchelkina, Z. V.; Sadovskii, M. V. *JETP Lett.* **2008**, *88*(8), 543.
(5) Chu, C. W.; Chen, F.; Gooch, M.; Guloy, A. M.; Lorenz, B.; Lv, B.; Sasmal, K.; Tang, Z. J.; Tapp, J. H.; Xue, Y. Y. *Phys. C* **2009**, *469*, 326.
(6) Gooch, M.; Lv, B.; Tapp, J. H.; Tang, Z.; Lorenz, B.; Guloy, A. M.; Chu, C. W. *EPL* **2009**, *85*, 27005.
(7) Parker, D. R.; Pitcher, M. J.; Baker, P. J.; Franke, I.; Lancaster, T.; Blundell, S. J.; Clarke, S. J. *Chem. Commun.* **2009**, *16*, 2189.
(8) Kurmaev, E. Z.; McLeod, J.; Skorikov, N. A.; Finkelstein, L. D.; Moewes, A.; Korotin, M. A.; Izyumov, Y. A., Clarke S. arXiv:0903.4901v1.
(9) Rotter, M.; Tegel, M.; Johrendt, D. *Phys. Rev. Lett.* **2008**, *101*, 107006.
(10) Christianson, A. D.; Goremychkin, E. A.; Osborn, R.; Rosenkranz, S.; Lumsden, M. D.; Malliakas, C. D.; Todorov, I.; Claus, H.; Chung, D. Y.; Kanatzidis, M. G.; Bewley, R. I.; Guidi, T. *Nature* **2008**, *456*, 930.
(11) Sasmal, K.; Bing, L.; Lorenz, B.; Guloy, A. M.; Chen, F.; Xue, Y.-Y.; Chu, C.-W. *Phys. Rev. Lett.* **2008**, *101*, 107007.
(12) Chen, G. F.; Li, Z.; Li, G.; Hu, W. Z.; Dong, J.; Zhang, X. D.; Zheng, P.; Wang, N. L.; Luo, J. L. *Chin. Phys. Lett.* **2008**, *25*, 3403.
(13) Juza, R.; Langer, K. *Z. Anorg. Allg. Chem.* **1968**, *361*, 58.

Published on Web 06/03/2010

defining the relationship between T_c and doping states.[14−16] Extensive investigations with high-resolution neutron diffraction and synchrotron X-ray diffraction in conjunction with elemental analysis on the composition of LiFeAs could not successfully resolve this issue.[14] Two samples prepared with nominal compositions of "$Li_{1.1}$FeAs" and "LiFeAs" showed superconducting transitions at different temperatures, 16 and 10 K respectively, although their structural refinements and determined chemical analyses were very similar at $Li_{0.86}$FeAs.[14] Separate studies on Li_{1-x}FeAs (x = 0, 0.2, 0.4) reported that T_c ranges from 16 K (LiFeAs) to 18 K ($Li_{0.6}$FeAs) with different x values but uncertainty in their actual stoichiometries.[15,16] A similar behavior was observed in samples of the isostructural Na_{1-x}FeAs of which T_c ranges from 9 to 18 K on different nominal compositions.[5,7] It is noticeable in both Li and Na samples that the T_c was defined by a broad superconducting response from less than 10% fraction of the sample measured. Based on these results, a question arises on whether the fully stoichiometric phase (i.e., NaFeAs) is in fact superconducting or not and whether the superconducting response depends on the content of alkali ion (i.e., degree of oxidation of [FeAs] layer).

To shed light on the superconductivity/composition issue in the NaFeAs system, we performed extensive analyses and "soft" chemical manipulations on the compound. In this report, we discuss the synthesis, chemical transformations, single crystal, and powder X-ray diffraction studies, magnetization, transmission electron microscopy (TEM), Mössbauer spectroscopy studies, and elemental analysis by inductively coupled plasma spectroscopy (ICP) on "as-prepared" and water- and air-exposed NaFeAs samples. We show that a slow deintercalation of Na^+ takes place on exposure to moisture or water, resulting in a gradual contraction of the unit cell and an increase of T_c from 9 K up to 25 K. On the other hand, a fast extraction of half the Na^+ ions from the interlayer space occurs in dry air which results in a change of the FeAs layer stacking and a phase change. Namely, a structural transformation from NaFeAs (PbFCl-type) to $NaFe_2As_2$ ($ThCr_2Si_2$-type) occurs and is accompanied by a T_c change from 9 to 12 K.

Experimental Section

Synthesis. All manipulations of materials were done in a nitrogen-filled glovebox with moisture and oxygen levels less than 0.2 ppm. The starting material FeAs was prepared by stoichiometric amounts of Fe (Cerac, powder, 99.9%; 2.1354 g) and As (Alfa Aesar, powder, 99.99%; 2.8646 g) placed in a fused silica ampule and subsequently sealed under reduced pressure of 1×10^{-4} Torr. The mixture was heated to 650 °C for 12 h, held there for a period of 6 h, and then heated to 1050 °C for 12 h, followed by cooling to room temperature for 12 h. The resulting product was a gray polycrystalline powder.

NaFeAs was synthesized by a solid-state diffusion reaction of Na and FeAs. Na (Aldrich, lump 99%; 0.0919 g, 4 mmol) and FeAs (0.522 g, 4 mmol) were placed in a Nb ampule that was sealed under an argon atmosphere and placed in an evacuated silica ampule. This assembly was heated at 800 °C with a rate of 60 °C/h, held there for 48 h and cooled down with the same rate. The purity of the final product was confirmed by powder X-ray diffraction, PXRD. No impurity phases were detected.

Elemental Analysis. Inductively coupled plasma optical emission spectroscopy was used for sample analysis. A Varian VISTA-MPX CCD Simultaneous ICP-OES instrument was used for the quantitative analysis. A stock solution of 100 ppm of each element (Na, Fe, and As) in 100 mL of ultra pure water was prepared by diluting 1000 ppm of Na (Fluka Chemicals ICP standard solution), 1000 ppm of Fe (GFS Chemicals ICP standard solution), and 1000 ppm of As (RICCA Chemicals ICP standard solution). Five concentrations were made for the calibration curve from the stock solution (serial dilution) of 5, 10, 20, 40, and 60 ppm (in 25 mL of ultra pure water).

An "as-prepared" NaFeAs sample (35 mg) was dissolved in 1 mL of aqua regia (3 parts of HCl and one part of HNO_3) and diluted in 250 mL of ultra pure water. Water-soaked samples (30 mg each) were treated in water for 4 days and more than 3 weeks (referred to as "supersoaked"), respectively. They were washed with copious amounts of ultra pure water before being dissolved in acid (using the same preparation method described above) before analysis. The compositions obtained from ICP analysis were $Na_{1.018(6)}Fe_{1.055(5)}As_{1.002(5)}$ for the "as-prepared" sample, $Na_{0.787(6)}Fe_{1.055(5)}As_{1.002(5)}$ for the sample soaked in water for 4 days, $Na_{0.681(6)}Fe_{1.067(5)}As_{1.004(5)}$ for the supersoaked sample.

Structure Determination. Single crystals of NaFeAs mounted on a glass fiber were collected on a STOE image plate diffractometer using graphite-monocromatized MoKα radiation. Details on the structure determination, final atomic positions, displacements parameters, anisotropic displacement parameters, and selected bond distances and angles are given in Table 1 and in the Supporting Information. It is important to point out that the refined compositions of the compound from all refinements of the structure (based on the data sets collected on different crystals selected from different reactions, namely "$Na_{1.2}$FeAs","NaFeAs", and "$Na_{0.86}$FeAs", were virtually identical, within a standard error of 2σ. Furthermore, the unit-cell parameters determined from the different data sets collected at room temperature were within 5σ each other. This confirmed that (a) the compound is a line compound, i.e., phase having compositional field narrower than about 1 at % and appearing as lines in binary phase diagram, and (b) the compositions from refined structures are indeed very close to NaFeAs.

High-resolution synchrotron powder diffraction data were collected using beamline 11-BM at the Advanced Photon Source (APS), Argonne National Laboratory, using an average wavelength of 0.458712 Å. Discrete detectors covering an angular range from −6 to 16° (2θ) were scanned over a 34° (2θ) range, with data points collected every 0.001° (2θ) and scan speed of 0.01°/s. For a detailed description of the instrument, see the Supporting Information.

Powder X-ray diffraction patterns were collected on Philips PANanlaytical diffractometer (Cu Kα radiation operating at 45 kV and 40 mA) on the samples as exposed in air during data collection (0.5 h). Separate data using STOE X-ray diffractometer (Mo Kα radiation operating at 50 kV and 40 mA) were collected on the powder samples sealed in capillary to avoid air exposure during data collection.

Magnetization. The magnetization measurements were performed in a noncommercial SQUID magnetometer described

(14) Pitcher, M. J.; Parker, D. R.; Adamson, P.; Herkelrath, S. J. C.; Boothroyd, A. T.; Clarke, S. J. *Chem. Commun.* **2008**, 5918–5920.
(15) Tapp, J. H.; Tang, Z.; Lv, B.; Sasmal, K.; Lorenz, B.; Chu, P. C. W.; Guloy, A. M.. *Phys. Rev. B* **2008**, *78*, 060505–1−5.
(16) Wang, X. C.; Liu, Q. Q.; Lv, Y. X.; Gao, W. B.; Yang, L. X.; Yu, R. C.; Li, F. Y.; Jin, C. Q. *Solid State Commun.* **2008**, *148*, 538–540.

elsewhere.[17] The earth magnetic field was reduced by a μ-metal shield to less than 0.01G. The magnetic moments were measured on warming in a field of typically 1G after initially cooling the sample in zero field to the lowest temperature. The sample preparation and measurements were performed at the same condition for all samples.

For evaluation of the volume fraction and transition temperature of superconducting phase in "as-prepared" samples with nominal compositions of "$Na_{1.2}FeAs$", "NaFeAs", and "$Na_{0.86}FeAs$", equal amounts (20 mg) of each sample were sealed in a nonmagnetic stainless steel capsule under nitrogen and measured. For investigation of superconducting behavior of NaFeAs in water, 20 mg of "NaFeAs" was carefully placed in a nonmagnetic stainless steel capsule on top of 2 drops of water under nitrogen. The capsule was sealed with a nonmagnetic stainless cap and measured as a function of time. The capsule was at room temperature in between measurements.

Bulk magnetic susceptibility measurements of NaFeAs polycrystalline samples were performed using a Quantum Design MPMS SQUID magnetometer in the temperature range between 5 and 300 K. Powder of each sample was mounted in a gel capsule and supported on a plastic straw. Temperature-dependent data were collected for both zero-field-cooled (ZFC) and field-cooled modes (FC) between 2 and 300 K, with an applied field of 500 G. No background correction for the sample holder (straw and gel capsule) was performed.

pH Measurements. 0.5408 g of NaFeAs was soaked in 0.020 L of deionized water. The pH was monitored with an Accumet portable AP61 pH meter. It consists of a measuring electrode, a reference electrode, and an automatic temperature-compensated (AT_c) unit that are built into a single housing. The measuring electrode is located in the center of the probe and the Ag/AgCl reference electrode and the ceramic junction are in the outer annular compartment. The pH meter was calibrated with standard buffer solutions before the experiment. The pH of the sample solution was measured in air immediately after immersing the solid material in water, followed by measurements after the elapse of 1, 6, 18, 23, 26, 40, 57, 62, 80, 86, and 134 h. The electrode was washed with deionized water before and after each measurement. In a subsequent measurements, 0.200 g of NaFeAs was soaked in 0.025 L of deoxygenated water and high-purity dry N_2 gas was bubbled throughout the entire measurements. The pH data were corrected for volume change due to water evaporation. The elapse of measurements was as follows: 1, 2, 3, 4, 5, 24, 27, 28, 29, 30, 50, 51, 52, 74, 75, 76, 77, 89, 90, 91, 95, 97, 110, 111, 115, 117, 120, 136, and 139 h.

Mössbauer Measurements. ^{57}Fe Mössbauer spectra (MS) were collected using a constant acceleration spectrometer equipped with a ^{57}Co(Rh) source kept at room temperature (RT). The spectrometer was calibrated with metallic Fe at RT and the isomer shift (IS) values were expressed relative to this standard. A closed loop He cryostat (ARS) was used for the low-temperature measurements. The samples "as-prepared" were very carefully handled not to expose them to air throughout whole procedures. The air-exposed samples were prepared by exposing the "as-prepared" samples in air for 24 h.

Transmission Electron Microscopy. NaFeAs samples ("as-prepared" and soaked in water for 3 h) were investigated using a JEOL 2100F transmission electron microscope (TEM) operating at a 200 keV accelerating voltage. Simulated electron diffraction patterns were conducted with the Mac Tempas program code (HRTEM Image Simulation Software Package. http://www.totalresolution.com). TEM samples were prepared by two different methods: NaFeAs powder was crushed under alcohol for "as-prepared" sample and water for water soaked sample, and a small amount of powder was placed on an amorphous carbon grid; G-1 epoxy was mixed with NaFeAs powder and the mixture was transferred into brass tube, cured at 111 °C. The tubes were cut into the required thickness, ground, dimpled, polished, and subsequently Ar-ion milled on a stage cooled with liquid nitrogen.

(17) Claus, H.; Welp, U.; Zheng, H.; Chen, L.; Paulikas, A. P.; Veal, B. W.; Gray, K. E.; Crabtree, G. W. *Phys. Rev. B* **2001**, *64*, 144507.

Results and Discussion

Synthesis and Structure. NaFeAs appears to have a very small stoichiometry width within the synthesis conditions employed in this study including starting materials, heating profile, and additional Na added in the reactions. The heating temperatures were varied between 600 and 850 °C. Dwelling times were varied from 2 h to 1 week and heating and cooling rates were between 50 and 70 °C/h. When the starting mixtures are heated at temperatures lower than 750 °C or higher than 800 °C with dwelling times longer than 2 days, the products included impurities of Na_3As, Fe_2As, and Fe. When elemental mixtures of Na, Fe and As were used as starting materials and reaction temperatures ~800 °C with dwelling times of 2 days, the products contained a small amount of air sensitive Na_3As. Pure product was obtained only when FeAs and Na were used as starting materials with a reaction temperature between 750 and 800 °C with dwelling time no longer than 2 days. Annealing NaFeAs over 700 °C for several days led to decomposition to binary phases and Fe, suggesting that the compound is incongruently melting.

NaFeAs crystallizes in the anti-PbFCl type structure with space group $P4/nmm$, $a = 3.9463(6)$ Å and $c = 7.0408(14)$ Å. The structure features anti-PbO type $[Fe_2As_2]^{2-}$ layers separated by Na^+ ions, Figure 1a. Na cations are in a square-based pyramidal coordination. The Fe−As bond distance is 2.435(1) Å, whereas the As−Fe−As bond angles are 108.21(6) and 110.11(3)° in agreement with literature values.[7] The $FeAs_4$ tetrahedra in the $[Fe_2As_2]^{2-}$ layers of NaFeAs are compressed along the c axis, whereas in LiFeAs the corresponding tetrahedra are compressed in the basal ab plane.

Water and Air Treatments. A remarkable observation that needs to be stressed is the rise of T_c when the NaFeAs is treated with water, in agreement with a recent report.[5] We found that water treated NaFeAs does not decompose but rather slowly reacts with it to oxidatively deintercalate Na^+ ions, see eq 1. When NaFeAs is soaked in deoxygenated water under an inert atmosphere for 5 weeks (supersoaked), the product still shows the NaFeAs structure as the major phase with only a small amount of a new phase, which was later shown to be $NaFe_2As_2$, see inset in Figure 2.

The content of Na^+ ion extracted from NaFeAs upon contact with water was monitored over time with a pH meter. As the Na ions are oxidatively deintercalated from the sample we expect a rise in pH based on the reaction of eq 1. The evolution of hydrogen suggested by eq 1 is

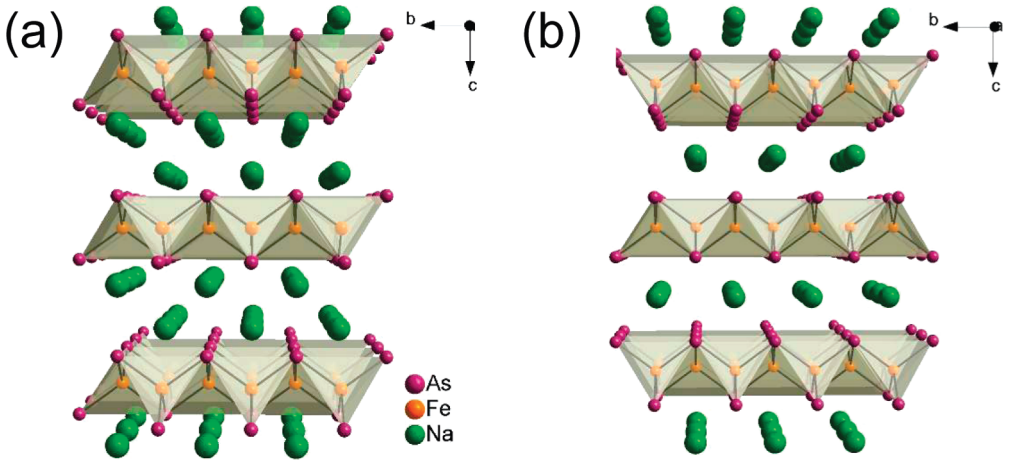

Figure 1. Projection of the structures of (a) NaFeAs and (b) $NaFe_2As_2$ along the *a*-axis.

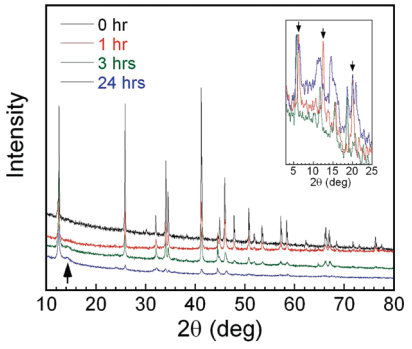

Figure 2. Powder diffraction patterns of NaFeAs before and after water treatment: before water treatment (black), 1 h in water (red), 3 h in water (green), 24 h in water (blue). The arrow represents the calculated position of the (001) peak of $NaFe_2As_2$. Inset: Powder diffraction patterns of capillary-sealed (no air contact) samples of NaFeAs "as-prepared", $NaFe_2As_2$ air oxidized, NaFeAs oversoaked in water, which shows presence of $NaFe_2As_2$ phase in the oversoaked sample.

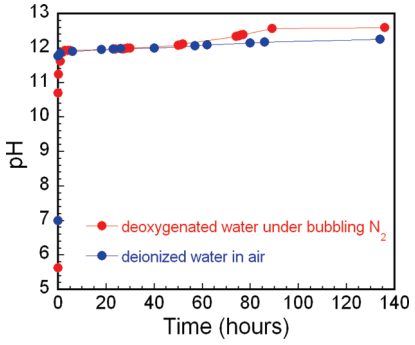

Figure 3. pH measured on water containing NaFeAs as a function of soaking time.

consistent with the gas bubbles observed upon contact of NaFeAs with water.

$$NaFeAs + xH_2O \rightarrow Na_{1-x}FeAs + xNaOH + x/2H_2 \quad (1)$$

Figure 3 shows the measured pH changes as a function of soak time. The first measurement made immediately after addition of NaFeAs in water shows a large sudden increase of pH from 7 to 11.8, indicating extremely fast initiation of oxidation followed by a slower increase afterward. To clarify whether or not oxygen dissolved in water plays a role in Na extraction, we performed two separate experiments with deionized water (presumably containing dissolved oxygen) and oxygen-free deionized water which was prepared by bubbling nitrogen gas before and throughout the entire measurement. As shown in Figure 3 the outcome of these experiments was very similar, indicating that the steep initial pH increase has to do more with reaction of NaFeAs with water rather than any oxygen dissolved in water. After 80 h in water, the x value in eq 1 is calculated as ~0.09 and the proposed formula of the water treated sample is $Na_{0.91}FeAs$. The standard error in these calculations is ±10%.

$$2NaFeAs + 1/2O_2 + H_2O \rightarrow NaFe_2As_2 + NaOH + 1/2H_2O_2 \quad (2)$$

When NaFeAs is exposed to air, we observed that the deficient $Na_{1-x}FeAs$ phase is bypassed and an oxidative transformation to $NaFe_2As_2$ ($ThCr_2Si_2$-type) begins immediately, eq 2. This indicates that NaFeAs is oxidized and deintercalated in two different pathways depending on the media. It retains the original PbFCl structure type in water while it transforms to the $ThCr_2Si_2$ structure type in air (or oxygen). In the presence of oxygen, half of the Na^+ ions are extracted from the interlayer space between the $[Fe_2As_2]^{2-}$ layers. This large loss of cations from the interlayer space creates unfavorable interlayer interactions which cause the FeAs layers to slide against each other to achieve better packing thereby adopting the $ThCr_2Si_2$ structure type, Figure 1b. The resulting $NaFe_2As_2$ is a metastable or a kinetically stabilized compound because the size of Na^+ is too small for the interlayer pockets of the $ThCr_2Si_2$ structure type. These pockets prefer larger cations such as K^+, Sr^{2+}, Ba^{2+}, and Cs^+.[11,18] The $NaFe_2As_2$ phase therefore cannot be directly synthesized at high temperature with solid-state

(18) Alireza, P. L.; Ko, Y. T. C.; Gillett, J.; Petrone, C. M.; Cole, J. M.; Lonzarich, G. G.; Sebastian, S. E. *J. Phys.: Condens. Matter* **2009**, *21*, 012208.

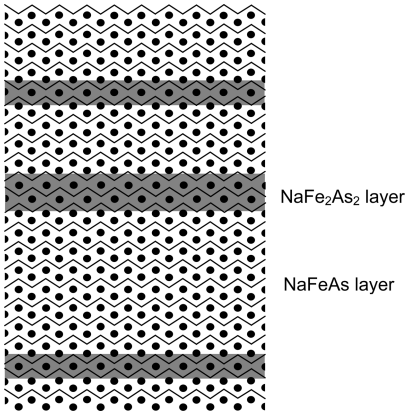

Figure 4. Schematic representation of the layer structure of a $Na_{1-x}FeAs$ sample after water treatment showing intergrowth of NaFeAs (major component) and $NaFe_2As_2$ (minor component) layers.

reactions. It can be obtained, however, in high yield by a controlled soft chemical reaction at 120 °C.[19] The occupancy of Na atoms in the structure was determined through single-crystal X-ray diffraction refinements of data collected on the several crystals obtained with different nominal compositions ("$Na_{1.2}FeAs$", "NaFeAs", and "$Na_{0.86}FeAs$"). The refined Na occupancies for all crystals studied were consistently close to 1 ($x \sim 0$) regardless of the x value in $Na_{1-x}FeAs$ obtained from elemental analysis and the pH measurements. This was surprising because we expected the value of x determined from crystallographic refinement and elemental analysis of the $Na_{1-x}FeAs$ samples to be very similar. One can speculate this discrepancy as follows. Since the phase transformation of NaFeAs into $NaFe_2As_2$ initiates immediately in air, we expect that the oxidative deintercalation process is not homogeneous. Instead of forming crystals of $Na_{2-y}Fe_2As_2$ (or $2Na_{1-x}FeAs$) in water (a weaker oxidant than oxygen), two phases form (probably intergrown) such as $(Na_2Fe_2As_2)_{1-y}(NaFe_2As_2)_y$ with $Na_2Fe_2As_2$ (i.e., NaFeAs) being the major component. A model for this type of intergrowth is shown in Figure 4. The majority $Na_2Fe_2As_2$ component dominates in the X-ray diffraction while the minority $NaFe_2As_2$ component contributes little. Therefore, the structure refinement based on the Bragg reflections "sees" only the stoichiometric NaFeAs (i.e., $x \approx 0$). The x value therefore in superconducting "$Na_{1-x}FeAs$" seems to be accounted for by the $(Na_2Fe_2As_2)_{1-y}(NaFe_2As_2)_y$ model (Table 1).

The difference in intra- and interlayer distances between neighboring As atoms in the NaFeAs and $NaFe_2As_2$ structures is significant.[20] In NaFeAs ($P4/nmm$), the intralayer As−As distances are 3.946(1) and 3.993(1) Å and the interlayer distance is 5.030(1) Å. In $NaFe_2As_2$ ($I4/mmm$), the corresponding intralayer As···As distances are 3.697(1) and 3.823(1) Å, respectively, whereas the interlayer As···As distance has contracted considerably to 3.628(1) Å. Compared to the NaFeAs structure, the Fe−As bonding in $NaFe_2As_2$ is stronger and there are possibly significant interlayer As···As interactions. The As···As interlayer distance is slightly less than the sum of the van der Waals radii of two As atoms (3.7 Å). This effect is reminiscent of the pressure induced superconductivity observed in undoped materials.[21] For example the interlayer distance of $CaFe_2As_2$ ($T_c \approx 10$ K at 0.69 GPa) is 3.8118(8) Å. Under pressure, it undergoes a so-called "volume collapse" with drastic reduction of its c-axis parameter by 9.5%. Thus, the interlayer distance becomes 3.4496(8) Å, which is below the sum of the van der Waals radii of two As atoms.

Table 1. Crystal Data and Structure Refinement for NaFeAs

empirical formula	NaFeAs
formula weight	153.76
T (K)	293(2)
wavelength (Å)	0.71073
cryst syst	tetragonal
space group	$P4/nmm$
a (Å)	3.9463(6)
b (Å)	3.9463(6)
c (Å)	7.0408(14)
V (Å^3)	109.65(3)
Z	2
density (calcd) (Mg/m^3)	2.329
absorp coeff (mm^{-1})	10.785
F(000)	70
cryst size (mm^3)	0.04 × 0.035 × 0.01
θ range for data collection (deg)	5.79−31.60
index ranges	$-5 \le h \le 5, -5 \le k \le 5, 0 \le l \le 10$
no. of reflns collected	621
independent reflns	136 [R(int) = 0.0775]
completeness to θ = 31.60°	99.3%
refinement method	full-matrix least-squares on F^2
data/restraints/params	136/0/9
GOF on F^2	1.827
final R indices [$I > 2\sigma(I)$][a]	R_1 = 0.0324, wR_2 = 0.1079
R indices (all data)[a]	R_1 = 0.0359, wR_2 = 0.1085
largest diff. peak and hole (e Å^{-3})	2.122 and −1.385

[a] $R_1 = [\sum||F_o|-|F_c||]/\sum|F_o|$. $wR_2 = \{\sum[w(|F_o|^2-|F_c|^2)^2]/\sum[w(|F_o|^4)]\}^{1/2}$ and $w = 1/(\sigma^2(I) + 0.0016I^2)$.

The contraction in the dimensions of the $[Fe_2As_2]$ layers of water-soaked samples was confirmed by TEM, indicating that Na ions are extracted from NaFeAs, see Figure 5. The cell parameters of NaFeAs shrink from a = 3.94(3) Å and c = 7.04(5) Å to a = 3.86(5) Å and c = 6.69(6) Å. The contraction of unit-cell parameters of the water-soaked NaFeAs was also observed in the high energy X-ray diffraction data collected on the 11-BM line at the Advanced Photon Source (APS) (see the Supporting Information). Na occupancies calculated by the Rietvelt refinement of the high energy X-ray diffraction data was 0.980(8) for "as-prepared" NaFeAs and 0.944(11) for the 24 h water-soaked sample.

A similar example of superconductivity in iron pnictide materials induced by water and unit cell contraction was reported on a $SrFe_2As_2$ epitaxial film[22] with $T_c \sim 25$ K while we were studying on NaFeAs. However, the origin of superconductivity in the report is, unlike our case,

(19) Tang, Z.; Lv, B.; Guloy, A. M.; Lorenz, B.; Xue, Y.; Chu, P. C. W. *The North American Solid State Chemistry Conference Program Abstract*; Columbus, OH, June 17−22, 2009; p 39.

(20) Cell parameters for NaFeAs and $NaFe_2As_2$ were taken from data collected on 11-BM beam line and atomic positions for NaFeAs were taken from single crystal X-ray data refinements. The cell parameters and atomic coordinated of KFe_2As_2 where used as initial values for the refinement of the isostructural $NaFe_2As_2$ phase. The parameters for KFe_2As_2 where taken from the Inorganic Crystal Structure Database (ICSD # 31473).

(21) Chu, C. W.; Lorenz, B. arXiv:0902.0809v1.

(22) Hiramatsu, H.; Katase, T.; Kamiya, T.; Hirano, M.; Hosono, H.. *Phys. Rev. B* **2009**, *80*, 052501.

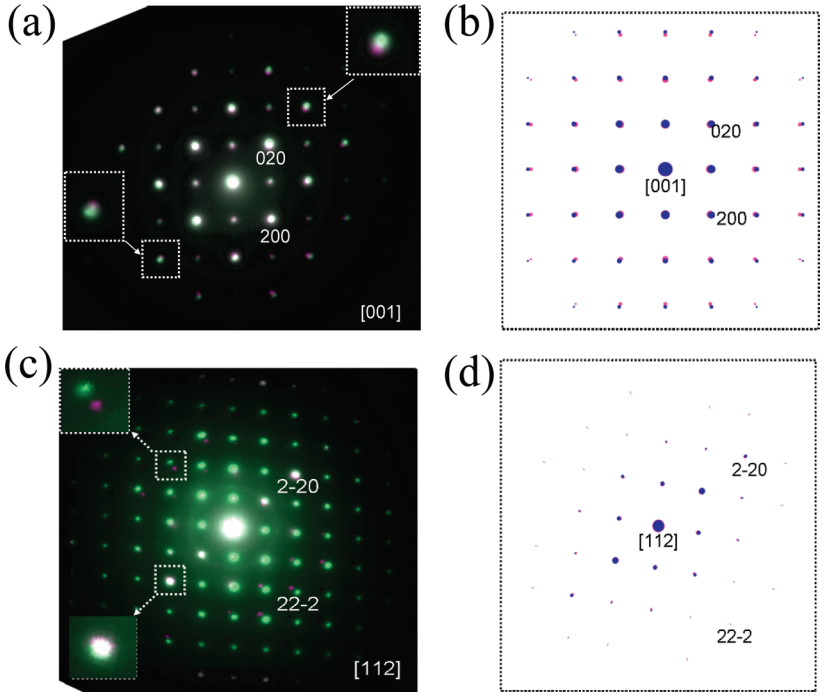

Figure 5. (a, c) Electron diffraction patterns for "as-prepared" (purple) and 3 h water-treated (green) NaFeAs samples along the zone axis [001] and [112], respectively. The insets in images a and c, the enlarged images corresponding to boxed regions, clearly show the spot splits that indicate the cell contraction of water treated sample. (b, d) Simulated electron diffraction for "as-prepared" (purple) and 9 h water treated (blue) using measured lattice parameters based on electron diffraction in a and c, respectively. The split of indexed $22\bar{2}$ reflection is larger than that of $2\bar{2}0$, indicating that lattice parameters shrink larger along the *c* direction than the *a*/*b* direction.

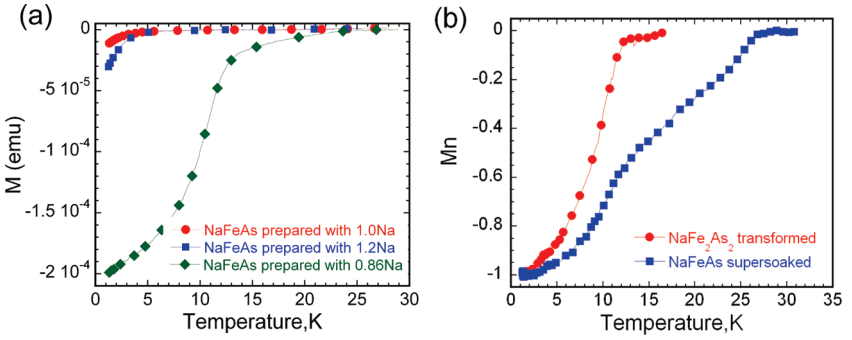

Figure 6. (a) Magnetization data for three NaFeAs samples prepared with the nominal compositions of NaFeAs, $Na_{1.2}FeAs$, and $Na_{0.86}FeAs$ and (b) normalized magnetization data for a NaFeAs sample transformed to $NaFe_2As_2$ by air exposure for 2 days and a NaFeAs sample supersoaked in water for 3 weeks.

suggested by encapsulation of oxygen atoms in interstitial sites of $[Fe_2As_2]$ layers.

Magnetization. Pristine samples of NaFeAs prepared with the nominal composition of "$Na_{1.2}FeAs$" and "NaFeAs" showed superconductivity around ~4 K with a very weak transition, see Figure 6a. The superconducting fraction in these two samples is very small, which is consistent with literature reports.[5,7,14] This suggests that stoichiometric NaFeAs is in fact nonsuperconducting and an adventitiously small fraction of $Na_{1-x}FeAs$ phase or a partially oxidized $(NaFeAs)_{1-y}(NaFe_2As_2)_y$ material included in the samples is responsible for the superconductivity. The Na-deficient compositions, $Na_{1-x}FeAs$ and $NaFe_2As_2$, could arise from inadvertent exposure to air or moisture during handling. The proposal that strictly stoichiometric NaFeAs is nonsuperconducting is supported by the DFT calculation on NaFeAs.[23] This is also corroborated by the fact that the filled isoelectronic analogue NdFeAsO is also nonsuperconducting while the oxygen deficient $NdFeAsO_{1-\delta}$ exhibits superconductivity.[24] In practice, because of the air sensitivity of NaFeAs phase it is very difficult to obtain 100% pure stoichiometric NaFeAs unless meticulous care is taken to exclude oxygen and moisture during handling over the entire process of characterization as well as synthesis. This difficulty accounts for the disparate reports of superconductivity of NaFeAs in the literature. The Na-deficient impurity phase showing superconductivity is very easily overlooked in X-ray powder diffraction diagrams

(23) Jishi, R. A.; Alyahyaei, H. M. *Adv. Condens. Matter Mater. Phys.* **2010**, 804343, and references therein .

(24) Takeshita, N.; Yamazaki, T.; Iyo, A.; Eisaki, H.; Kito, H.; Ito, T.; Hirayama, K.; Fukazawa, H.; Kohori, Y. *J. Phys. Soc. Jpn.* **2008**, *77*, 131.

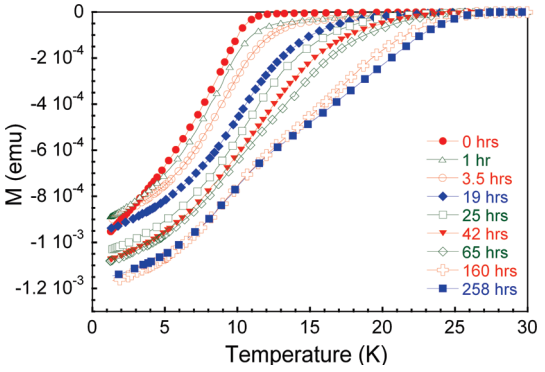

Figure 7. Bulk magnetization of NaFeAs as a function of soak time in water.

of polycrystalline samples as the characteristic (001) reflection (arrow in Figure 2) of $NaFe_2As_2$ appears as a negligible bump in NaFeAs samples reported previously.[7]

When NaFeAs is treated with water, an increase of T_c is observed with time until about 4 d reaching a maximum T_c of 25 K (optimal doping state). Further soaking in water causes transformation to $NaFe_2As_2$. The T_c values of air-oxidized $NaFe_2As_2$ and water treated NaFeAs as a function of soak time are given in Figures 6 and 7. It should be noted that all samples in Figure 6a have not been exposed to air or moisture, whereas the 0 h data in Figure 7 were obtained 5 min after placing the sample on top of 2 drops of water under nitrogen. The sudden rise of T_c as well as volume fraction of superconducting phase in the 0 h measurement is consistent with the pH experiment. This T_c dependence on doping of NaFeAs is similarly observed in other iron pnictides with pressure. When iron pnictides are underdoped, T_c increases with the applied pressure, whereas it remains approximately constant at optimally doped states and decreases when overdoped.[25]

Water-soaked samples of NaFeAs show almost temperature independent Pauli paramagnetic susceptibility. The susceptibility (molar χ_m) data can be described by $\chi_m = \chi_0 + C/(T - \Theta)$, where χ_0 is the temperature independent term (Pauli paramagnetism), C is the Curie constant, T is the temperature, and Θ is the paramagnetic Curie temperature. The effective magnetic moment (μ_{eff}) was calculated from $C = (N\mu_{eff}^2)/3k_b$, where N is Avogadro's number and k_B is Boltzmann's constant. The following parameters were derived from these fits: μ_{eff}/Fe = 0.27(5), 0.55(3), and 1.05(10) μ_B (μ_B = Bohr magneton) and $\Theta = -4(7)$, $-22(3)$, and $-44(10)$ K for the "as-prepared" sample, a sample soaked in water for 2 h, and a sample soaked over 10 days, respectively. Similarly, the T-dependence of $LaFeAs(O_{1-x}F_x)$ (x = 0.04) follows Curie–Weiss law between 30 and 200 K. The obtained Weiss temperature is Θ = 10.3 ± 2 K.[26] This suggests that the superconductivity in the F-doped $LaFeAs(O_{1-x}F_x)$ emerges when a magnetic ordering is suppressed. Furthermore, above the ordering temperature the magnetic susceptibility of FeTe falls off in a Curie–Weiss fashion.[27] The ordered magnetic moment in FeTe is large, ~2 μ_B, consistent with a localized S = 1 at every site. Given the metallic character of FeTe, this was explained by self-doping mechanism, i.e., some Fe atoms are occupying interlayer sites. In the case of NaFeAs "self-doping" occurs by extraction of Na cations from the layers upon reaction with moisture and/or oxygen from the air. The ordered magnetic moment of NaFeAs was found to be μ_{eff} = 0.1–0.2 μ_B per Fe from muon spin rotation measurements (μSR).[7] It appears that the effective magnetic moment of Fe increases with soak time. Studies of the magnetic interactions of the Fe moments performed by self-consistent spin spiral calculations for coplanar spin-spiral structures in $Ba_{1-x}K_xFe_2As_2$ and $LaO_{1-x}F_xFeAs$ with x = 0, 0.1, 0.2, 0.3 show that the hole doping of the FeAs layer by K or F substitution results in strong reduction of the stabilization energy of the magnetic solution. Thus, the calculated Fe moment for $Ba_{1-x}K_xFe_2As_2$ decreases from 1.34 μ_B in the undoped (x = 0) compound to 0.99 μ_B for x = 0.3.[27] In our case hole doping in the FeAs layers is introduced by extraction of some of the Na ions from the structure. Our experimental data, however, show that the magnetic moment increases with soaking time from the undoped "as-prepared" to the phases that presumably are more hole doped. The Fe magnetic moments in other iron pnictide superconductors determined by neutron powder diffraction are also very small, for instance, 0.35 μ_B in LaFeAsO,[28] 0.25 μ_B in NdFeAsO,[29] and 0.87 μ_B in $BaFe_2As_2$.[30,31] All values of μ_{eff} are smaller than expected for a three-dimensional Heisenberg system and this is a likely reflection of the layered nature of the structure.[32–34] Moreover, the presence of magnetic frustration and/or spin fluctuation has been suggested in order to interpret the reduced ordered moment in all FeAs-based superconductors.[28,35,36]

On the other hand, the air-exposed NaFeAs samples (i.e., converted to $NaFe_2As_2$) exhibit different behavior. The compound shows Pauli paramagnetic-like magnetic property with a broad superconducting transition at 10–13 K but does not follow Curie–Weiss law (see the Supporting Information), thus we could not extract the magnetic moments from the bulk molar magnetic susceptibility. It should be noted that there are no reports on magnetic susceptibility or magnetization of AFe_2As_2 (A = K, Rb, Cs). It is difficult to accurately determine magnetic properties of these phases because of possible inclusion of magnetic impurities. DFT calculations performed on KFe_2As_2 show

(25) Chu, C. W.; Lorenz, B. *Phys. C.* **2009**, *469*, 385–395.
(26) Nakai, Y.; Ishiday, K.; Kamihara, Y.; M., H.; Hosono, H. *J. Phys. Soc. Jpn.* **2008**, *77*, 073701.
(27) Imai, T.; Ahilan, K.; Ning, F. L.; McQueen, T. M.; Cava, R. J. *Phys. Rev. Lett.* **2009**, *102*, 177005.
(28) Yaresko, A. N.; Liu, G.-Q.; Antonov, V. N.; Andersen, O. K. *Phys. Rev. B* **2009**, *79*, 144421.
(29) de la Cruz, C.; Huang, Q.; Lynn, J. W.; Li, J.; Ratcliff, W., II; Zarestky, J. L.; Mook, H. A.; Chen, G. F.; Luo, J. L.; Wang, N. L.; Dai, P. *Nature* **2008**, *453*, 899.
(30) Chen, Y.; Lynn, W.; Li, J.; Li, G.; Chen, G. F.; Luo, J. L.; Wang, N. L.; Dai, P.; de la Cruz, C.; Mook, H. A., Phys. Rev. B **2008**, B *78*, 064515.
(31) Huang, Q.; Qiu, Y.; Bao, W.; Green, M. A.; Lynn, J. W.; Gasparovic, Y. C.; Wu, T.; Wu, G.; Chen, X. H. *Phys. Rev. Lett.* **2008**, *101*, 257003.
(32) Becerra, C. C.; Paduan-Filho, A.; Palacio, F. *J. Phys.: Condens. Matter* **2000**, *12*, 6207.
(33) Mills, D. L. *Phys. Rev. B* **1971**, *3*, 3887.
(34) Kumar, P. *Phys. Rev. B* **1974**, *10*, 2928.
(35) Yildirim, T. *Phys. Rev. Lett.* **2008**, *101*, 057010.
(36) Si, Q.; Abrahams, E. *Phys. Rev. Lett.* **2008**, *101*, 076401.

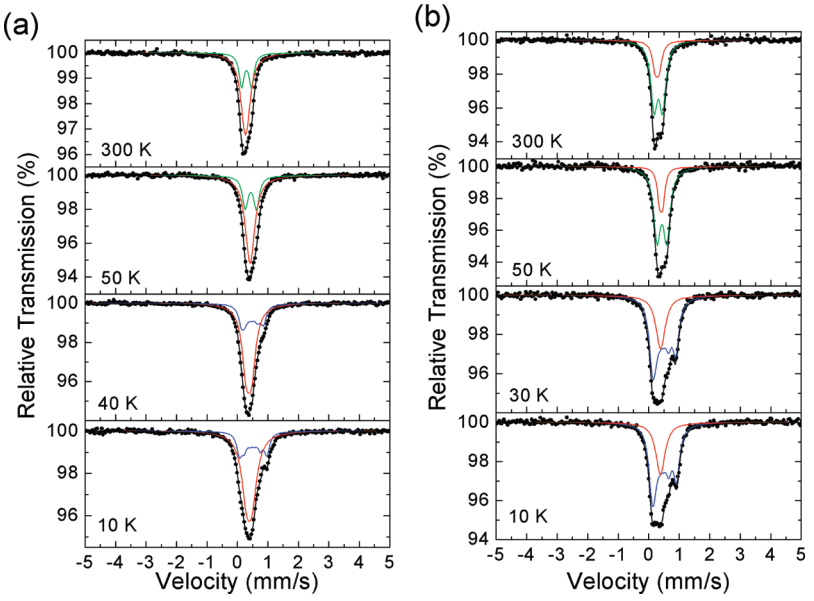

Figure 8. ^{57}Fe Mössbauer spectra of the two "as-prepared" samples recorded at different temperatures: (a) sample 1 and (b) sample 2. The colors correspond to the components described in the text: red (D1/D), green (D2), and blue (S).

a weak magnetic ground state, ferromagnetic in character, with moments of 1.1 μ_B/Fe.[37] Recent reports suggest that KFe_2As_2 is close to a Pauli paramagnet based on NMR measurements.[38]

Mössbauer Spectroscopy. NaFeAs was reported to undergo structural, electronic and magnetic transitions at low temperatures.[7,36−38] In particular, the magnetic transition detected ~40 K is proposed to involve a spin density wave (SDW) order.[37] The spins of the Fe ions order antiferromagnetically within the Fe−As layers at the $a-b$ plane and the interlayer magnetic interaction seems to be quite weak. In addition, as mentioned above, the Fe moment estimated from neutron diffraction experiments, is extremely low and of the order of 0.1−0.2 μ_B.[7,35] This means that a very low hyperfine magnetic field (B_{hf}) is expected in the MS of this compound below 40 K (see below).

Although a structural transition from tetragonal to orthorhombic occurs in the range of 45−50 K,[39−41] Fe occupies a single crystallographic tetrahedral As-coordinated site in both symmetries. Thus, one would expect the appearance of only one component in the MS of the NaFeAs samples, which should start to show a small hyperfine magnetic splitting below 40 K. However, the experiments on the NaFeAs samples by a first look seem to contradict this expectation.

In particular, the MS of the two "as-prepared" NaFeAs samples (sample 1 and sample 2, identical to "as prepared" with 1.0Na in Figure 6a) appearing in Figure 8, show the presence of at least two quadrupole doublets, D1 and D2, in the paramagnetic temperature region (40 K < T < 300 K). For temperatures below the magnetic transition at 40 K, the spectra can be fitted using a paramagnetic quadrupole doublet (D) and a magnetic sextet (S) with quite small B_{hf} values, of the order of 25−30 kOe, which correspond to the two components D1 and D2 of the paramagnetic temperature region. Moreover, we could even allow a very small B_{hf} of the order of 5−7 kOe to be present for the other so-called paramagnetic component D below 40 K, without disproving much the quality of the fits. However, the fits using the zero B_{hf} paramagnetic D component were of better quality.

Thus, we have used the model of one paramagnetic doublet D and one magnetic sextet S to adequately fit the spectra of the "as prepared" samples below 40 K. As Fe in NaFeAs occupies a single crystallographic site, each of these two components should therefore correspond to different "phases" in the samples. The relative spectral areas of the D and S components (see the Supporting Information, Table S4), which correspond to the amount of the Fe ions in each "phase" (whatever kind of "phase" it is) are different between the two "as prepared" samples. In particular for sample 1 which was exposed to air for a very brief period the fit gave ~70% for D and ~30% for S. For sample 2, which was handled with much greater care to avoid air exposure during the entire process of measurements, the fit showed ~25% for D and ~75% for S. Above 40 K, the fitting model of the two doublets D1 and D2, corresponding to the D and S components of the temperature area below 40 K, gave very similar results as regards their absorption areas.

The MS of the two samples after 24 h of air exposure, which results in a phase transformation to $NaFe_2As_2$, are given in Figure 9. A paramagnetic component (P), with Mössbauer parameters values very similar to the D/D1 components of the "as-prepared" samples dominates the

(37) Singh, D. *J. Phys. Rev. B* **2009**, *79*, 174520.
(38) Fukazawa, H.; Yamada, Y.; Kondo, K.; Saito, T.; Kohori, Y.; Kuga, K.; Matsumoto, Y.; Nakatsuji, S.; Kito, H.; Shirage, P. M.; Kihou, K.; Takeshita, N.; Lee, C.-H.; Iyo, A.; Eisaki, H. *J. Phys. Soc. Jpn.* **2009**, *78*, 083712.
(39) Ishida, K.; Yusuke, N.; Hideo, H. *J. Phys. Soc. Jpn.* **2009**, *78*, 062001.
(40) Chen, G. F.; Hu, W. Z.; Luo, J. L.; Wang, N. L. *Phys. Rev. Lett.* **2009**, *102*, 227004.
(41) Li, S.; Cruz, C. d. l.; Huang, Q.; Chen, G. F.; Xia, T.-L.; Luo, J. L.; Wang, N. L.; Dai, P. *Phys. Rev. B* **2009**, *80*, 020504.

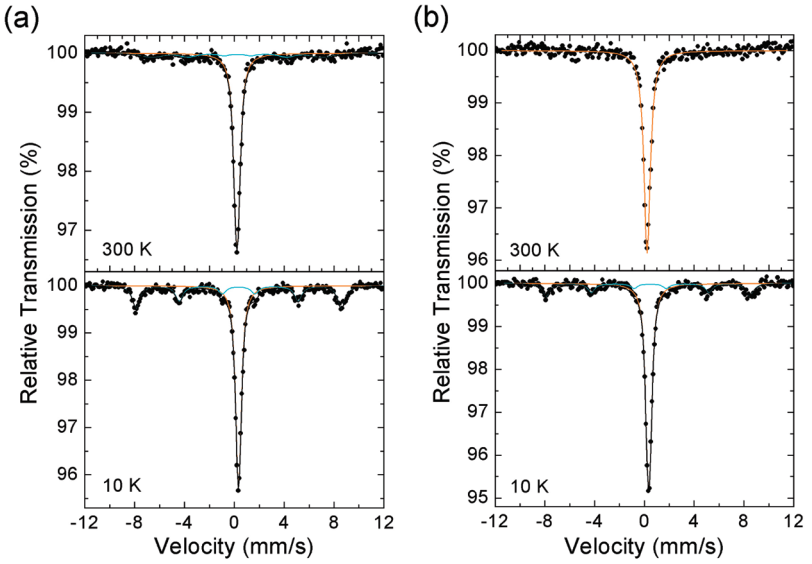

Figure 9. ^{57}Fe Mössbauer spectra of the two air exposed samples recorded at different temperatures: (a) sample 1 and (b) sample 2. The colors correspond to the components described in the text: orange (P) and light blue (O).

spectra of both air exposed samples. In addition, the magnetic sextet S with the very small B_{hf} value of the "as-prepared" samples is absent in the air exposed samples at 10 K and a new "oxidized" magnetic component (O) with large B_{hf}, on the order of 510 kOe, at the low temperature spectra of these samples appears. However, this O component possesses different absorption areas in the two air exposed samples, as its spectral area is ~38% for sample 1 and 24% for sample 2.

How are all these components interpreted according to the crystal and magnetic structure of NaFeAs? We believe that the appearance of two components instead of the one expected for the "as-prepared" samples is a consequence of the extreme sensitivity of the stoichiometric NaFeAs phase to moisture and oxygen which results in an intimate phase mixture of NaFeAs and $NaFe_2As_2$ as described above. As stated above, it is quite difficult to avoid even a very small amount of moisture from coming in contact with the sample creating Na deficiencies. However, these deficiencies are not so easily detected by powder X-ray diffraction study as they are probably not ordered, so they do not give rise to large peak-shifts, additional peaks or intensity changes in the corresponding diagrams. In addition, a previous report[5] connects these deficiencies with grain surface effects and even to the occurrence of superconductivity with the preferred absence of Na in the surface of the grains of the samples.

The above results indicate clearly that the so-called "as-prepared" samples are in fact two phase systems, with the D/D1 components corresponding to the first "phase" and the S/D2 components to the second "phase". The resemblance of the paramagnetic D/D1 and P components in "as-prepared" and air-exposed samples, respectively, leads us to propose that the D/D1 components, and consequently the first "phase" of the "as-prepared" samples, arises from the fraction of these samples with increased Na deficiencies ($Na_{1-x}FeAs$) because of their exposure in moisture or oxygen. As these components remain almost intact after air exposure, they correspond to the part of the samples which have already and unavoidably come in contact with air during handling. On the other hand, the disappearance of the S/D2 components from the spectra of the "as-prepared" samples, after air exposure, suggests the second "phase" is the stoichiometric NaFeAs part of these samples. This analysis is consistent with the increased amount of the second "phase" in the "as-prepared" sample 2, which was treated with much greater care as regards air exposure. Furthermore, the IS values of components D1 and D of the first Na-deficient "phase" are lower than those of components D2 and S, which correspond to the second more stoichiometric "phase", indicating a relative increase of the valence state of iron from the nominal Fe^{2+} in the formal $Na^{1+}Fe^{2+}As^{3-}$ configuration to higher values for the first "phase".

Finally, we propose that the O component originates from further oxidation of the Fe ions of the $NaFe_2As_2$ phase, which follows the transformation of stoichiometric NaFeAs after air exposure to $NaFe_2As_2$, as shown in reaction scheme below. However, this further oxidation seems to involve only a minority of the Fe ions, probably those situated mainly in the surface of the samples' grains, as the majority in both air exposed samples is represented by the P component, which corresponds to $NaFe_2As_2$ and the transformation to an iron oxide phase is thus restricted to only a small fraction of the samples.

$$\underset{\text{(as-prepared)}}{\text{NaFeAs (S)} + \text{Na}_{1-x}\text{FeAs (D)}} \xrightarrow[\text{air}]{} \underset{\text{(oxidized)}}{\text{NaFe}_2\text{As}_2\text{ (P, O)}}$$

Concluding Remarks

The structural, chemical, and physical properties of the NaFeAs system were further characterized. The chemical reactivity of this system is surprisingly high and complex.

Our data shows that superconductivity occurs when the material is Na deficient. Most importantly, we have observed a significant increase in T_c after exposure of the material to water and air. The T_c can be directly associated with the decrease of Na^+ in the material, which was shown by pH measurements and ICP elemental analysis. The extraction of Na^+ is accompanied by unit-cell contraction which is detected with synchrotron X-ray powder diffraction data and TEM. The oxidation of NaFeAs progresses differently in water and in air. It oxidizes slowly and slightly in water retaining the original anti-PbFCl structure and quickly and extensively in air (oxygen) transforming to the $ThCr_2Si_2$ structure type. The highest T_c was observed at 25 K from NaFeAs samples treated with water, which decreases to 12 K when the "overdoped" $NaFe_2As_2$ is obtained in air. This soft redox chemistry could be a useful approach to change the doping state of materials such as REOFeAs and (A/AE)Fe_2As_2. An electrochemically controlled approach to controlling this topotactic redox chemistry will also be attractive to access intermediate state of oxidation.

Acknowledgment. This research was supported by the U.S. Department of Energy, Office of Basic Energy Sciences, under Contract DE-AC02-06CH11357. Transmission electron microscopy work was performed in the (EPIC) (NIFTI) (Keck-II) facility of NUANCE Center at Northwestern University. The NUANCE Center is supported by NSF-NSEC, NSF-MRSEC, Keck Foundation, the State of Illinois, and Northwestern University.

Supporting Information Available: X-ray crystallographic data (CIF), structure determination, atomic positions, displacement parameters, anisotropic displacement parameters, magnetization, Mössbauer parameters of fitted spectra. This material is available free of charge via the Internet at http://pubs.acs.org.